Physics of the Earth and Planetary Interiors 176 (2009) 83–88

Contents lists available at ScienceDirect

Physics of the Earth and Planetary Interiors

journal homepage: www.elsevier.com/locate/pepi

# Electrical conductivity of pyrope-rich garnet at high temperature and high pressure

Lidong Dai [a,b], Shun-ichiro Karato [b,*]

[a] Laboratory for Study of the Earth's Interior and Geofluids, Institute of Geochemistry, Chinese Academy of Sciences, Guiyang, Guizhou 550002, China
[b] Department of Geology and Geophysics, Yale University, New Haven, CT 06520, USA

ARTICLE INFO

*Article history:*
Received 1 November 2008
Received in revised form 6 April 2009
Accepted 7 April 2009

*Keywords:*
Electrical conductivity
Pyrope garnet
Pressure
Frequency
Water

ABSTRACT

Garnet is one of the important constituent minerals in the upper mantle and the transition zone of the Earth's mantle. However, there were very few previous works on its electrical conductivity. We have measured the electrical conductivity of single crystal of pyrope-rich garnet ($\sim Py_{73}$-$Alm_{14}$-$Grs_{13}$) under the conditions of 4–16 GPa, 873–1473 K and frequency range from $10^{-2}$ to $10^{6}$ Hz, with a range of water content (from less than 10 to 7000 H/$10^{6}$ Si). A KAWAI-type multi-anvil apparatus and a Solarton-1260 Impedance/Gain Phase analyzer were used in this study. The impedance spectra showed two circles correspondent to the intrinsic resistivity of the crystal and to the effects of charge accumulation at the electrodes. The DC electrical conductivity was determined by the impedance spectroscopy. Molybdenum and molybdenum oxide solid buffer was used to control the oxygen fugacity. Results on hydrous and anhydrous samples were compared to determine the influence of water content on the electrical conductivity of single crystal garnet. Under anhydrous conditions, the electrical conductivity of garnet increases with temperature and decreases with pressure. When we used a thermal activation parameterization, we obtain the following relationship: $\sigma = A\exp(-(E^* + PV^*)/RT)$, $A = 1036(\pm 236)(1 - 0.044(\pm 0.007)P(\mathrm{GPa}))$ S/m or $A = \exp[7.16(\pm 0.37)(1 - 0.012(\pm 0.009)P(\mathrm{GPa}))]$ S/m, $E^* = 128 \pm 6$ kJ/mol and $V^* = 2.50 \pm 0.48$ cm$^3$/mol. Hydrous garnet crystals have significantly higher electrical conductivity with different temperature and pressure sensitivity, and the conductivity in these samples increases with the water content. The results can be summarized as $\sigma = A \cdot C_w^r \exp[-(E^* + PV^*)/RT]$ with $A = 1950$ (+870, −600) S/m, $r = 0.63 \pm 0.19$, $E^* = 70 \pm 5$ kJ/mol and $V^* = -0.57 \pm 0.05$ cm$^3$/mol. These results are similar to those obtained by Wang et al. [Wang, D.J., Mookherjee, M., Xu, Y.S., Karato. S., 2006. The effect of water on the electrical conductivity of olivine. Nature 443, 977–980] for olivine, Huang et al. [Huang, X.G., Xu, Y.S., Karato, S., 2005. Water content in the transition zone from electrical conductivity of wadsleyite and ringwoodite. Nature 434, 746–749] for wadsleyite and ringwoodite and we suggest that the mechanism of hydrogen conduction is likely common to these minerals. We conclude that hydrogen enhances the electrical conductivity of pyrope-rich garnet and its effect increases with pressure but decreases with temperature. At a typical pressure and temperature in the upper mantle, the influence of water is substantial.



## 1. Introduction

Results of experimental studies of the electrical conductivity of mineral and rock at high pressure and temperature provide an important means to infer the physical and/or chemical state of Earth's interior by comparing the geophysically inferred conductivity with laboratory-based data on the sensitivity of electrical conductivity on physical and/or chemical state of materials. In particular, a suggestion by Karato (1990) implies that the hydrogen content in Earth's interior may be inferred from electrical conductivity, which has stimulated the experimental studies on electrical conductivity with a special attention to the role of water (hydrogen) (e.g., Huang et al., 2005; Wang et al., 2006; Yoshino et al., 2006, 2008a,b).

However, such studies have not been conducted on pyrope or pyrope-rich garnet, an important constituent mineral in Earth's upper mantle. Furthermore, there have been some technical issues on the experimental methodology to determine electrical conductivity under hydrous conditions. For example, Yoshino et al. (2006, 2008a,b) reported results on electrical conductivity measurements on olivine, wadsleyite, ringwoodite and majorite garnet and concluded that the influence of hydrogen on electrical conductivity is small and geophysically inferred conductivity profiles in the upper

* Corresponding author at: Department of Geology and Geophysics, Yale University, New Haven, CT 06520, USA. Tel.: +1 203 432 3147; fax: +1 203 432 3134.
*E-mail address:* shun-ichiro.karato@yale.edu (S.-i. Karato).

0031-9201/$ – see front matter © 2009 Elsevier B.V. All rights reserved.
doi:10.1016/j.pepi.2009.04.002

**Table 1**
Chemical composition of sample (wt%).

| Oxides (wt%) | | | | | | | | | | |
|---|---|---|---|---|---|---|---|---|---|---|
| $Cr_2O_3$ | NiO | MnO | FeO | $Na_2O$ | $K_2O$ | $Al_2O_3$ | CaO | MgO | $TiO_2$ | $SiO_2$ |
| 3.98 | 0.01 | 0.34 | 7.42 | 0.03 | 0.02 | 21.51 | 5.13 | 20.82 | 0.07 | 41.81 |

mantle can be explained by factors other than a high hydrogen content. Yoshino et al.'s results for olivine, wadsleyite and ringwoodite are different from those by Huang et al. (2005) and Wang et al. (2006) who used somewhat different experimental technique which raises an issue of the validity of different techniques (Karato and Dai, in press).

Consequently, the purposes of the present study are (i) to provide a first data set on the electrical conductivity in garnet (pyrope-rich garnet) for a broad range of conditions including the influence of water and (ii) to explore the influence of different techniques to determine the conductivity. We will first present the experimental methods and results, and discuss the mechanisms of electrical conductivity and possible implications for the water in the upper mantle and transition zone.

## 2. Experimental methods

### 2.1. Sample preparation

We used single crystals of garnet collected at the Garnet Ridge, AZ, USA. The chemical composition of this garnet is shown in Table 1 and is approximately $Py_{73}$-$Alm_{14}$-$Grs_{13}$ that is close to a garnet in the pyrolite model (e.g., Ringwood, 1975). The water content of the original sample is less than ~10 H/$10^6$ Si. We call this "dry" garnet.

In order to prepare samples with higher water contents, we made hydrothermal annealing experiments at $P$ = 8 GPa, $T$ = 1573 K for 5 h using Mo–$MoO_2$ buffer to control the oxygen fugacity (here after called MMO buffer). The details of hydrothermal experiments are described by Mookherjee and Karato (in press). The FT-IR spectroscopy of hydrothermally treated samples showed homogeneously distributed hydrogen.

### 2.2. Sample characterization

In order to determine the water content of the samples, the infrared spectra of samples were obtained at wave-numbers from 1000 to 4000 $cm^{-1}$ both before and after each experiment. The measurements were made using a Fourier transform infrared spectroscopy (FT-IR) spectrometer (BIORAD, Varian 600 UMA). Doubly polished samples with a thickness of less than 100 μm were prepared for the IR analysis. The IR absorption of samples was measured by unpolarized radiation with a Mid-IR light source, a KI beam splitter and an MCT detector with a 100 μm × 100 μm aperture. Two hundred fifty-six times scans were accumulated for each sample. The infrared spectra of the acquired samples are shown in Fig. 1. We used the Paterson (1982) calibration to determine the water content from FT-IR absorption using,

$$C_{OH} = \frac{B_i}{150\xi} \int \frac{K(\nu)}{(3780 - \nu)} d\nu \quad (1)$$

where $C_{OH}$ is the molar concentration of hydroxyl (H/$10^6$ Si), $B_i$ is the density factor ($3.19 \times 10^4$ cm H/$10^6$ Si), $\xi$ is the orientation factor (1/2), and $K(\nu)$ is the absorption coefficient in $cm^{-1}$ at wave-number $\nu$ in $cm^{-1}$. The integration was made from 3000 to 3750 $cm^{-1}$.

The water content of the original sample is less than 10 H/$10^6$ Si (0.0001 wt% $H_2O$). Three samples with water contents of 0.047, 0.016 and 0.0046 wt% were obtained after hydrothermal annealing. The water loss during the electrical conductivity measurements of hydrous sample was less than 10%.

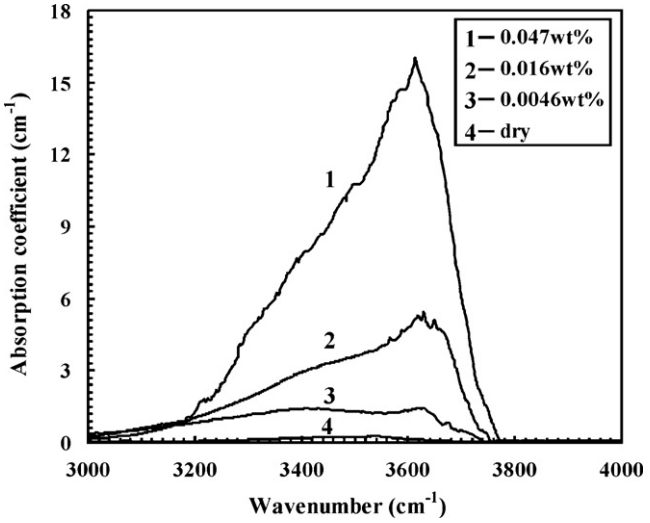


**Fig. 1.** FT-IR spectra of pyrope garnet for the wave-number range of 3000–4000 $cm^{-1}$.

### 2.3. Experimental methods and principles

The experimental sample assembly is shown in Fig. 2. Pressure was generated by eight cubic tungsten carbide anvils (26 mm × 26 mm × 26 mm) with an 8 or 11 mm truncated edge length. Pressure calibrations were made using the phase transitions of coesite and stishovite (Zhang et al., 1996, 9.5 GPa and 1573 K), as well as forsterite and wadsleyite (Morishima et al., 1994, 4 GPa and 1573 K). In order to avoid the influence of adsorbed water on the measurement of electrical conductivity, MgO was heated to 1273 K prior to sample assemblage. In order to control the oxygen fugacity of the sample chamber and reduce the leakage currents, a Mo foil shielding was placed between a sample and an MgO insulation tube. A disk-shaped sample (Ø 1.6 mm × 0.4 mm) was placed between two Mo electrodes that were surrounded by an alumina ring. The temperature was measured by a $W_{26\%}Re$-$W_{5\%}Re$ ther-

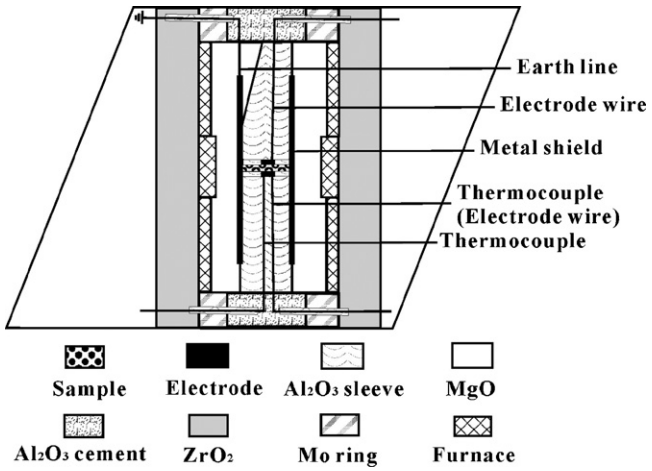


**Fig. 2.** Experimental setup for electrical conductivity measurements at high pressure and temperature.

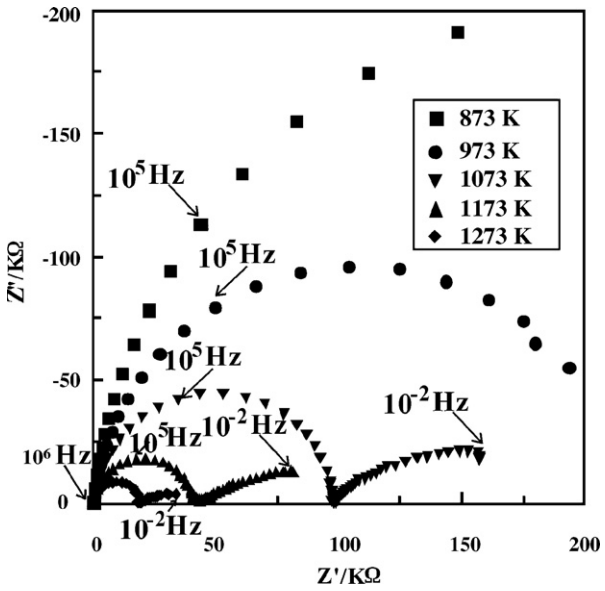


**Fig. 3.** A $Z'$ versus $Z''$ plot of complex impedance of hydrous garnet from $10^{-2}$ to $10^6$ Hz (right to left), obtained under conditions of 8.0 GPa, 873–1273 K and 0.0046 wt% water content. $Z'$ and $Z''$ are the real and imaginary part of complex impedance respectively. For low temperature results, only parts of whole spectra are shown.

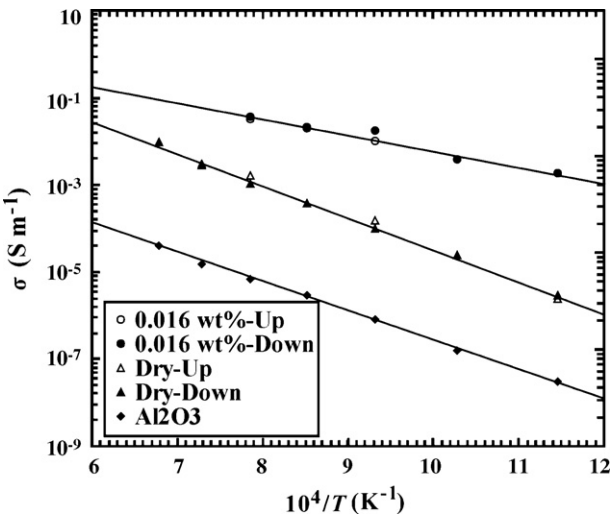


**Fig. 4.** Typical results of conductivity measurements showing the influence of temperature cycling. Shown together is the conductivity of alumina at 8.0 GPa. The influence of temperature cycling is minor and the resistance of alumina is much higher than samples.

mocouple that was placed on the surface of sample and used as one of the electrodes. The experimental errors of the temperature and pressure gradient were measured at less than 10 K and 0.5 GPa, respectively. The errors in electrical conductivity measurement through the impedance fitting were estimated to be no more than 5%.

The pressure was first raised at the rate of ~2.5 GPa/h to a designated pressure. Under a constant pressure condition, temperature was raised at the rate of ~100 K/min to the preset value and the impedance spectroscopy measurements were made at various temperatures. After the temperature reached to an each value for a constant pressure condition, the ZPlot program of a Solartron-1260 Impedance/Gain Phase analyzer was run to determine the complex impedance for the frequency range of $f = 10^{-2}$ to $10^6$ Hz for a voltage of 0.5 V. The impedance semi-circle arc of high frequency branch ($10^6$–$10^3$ Hz) was fitted by virtue of an equivalent circuit of the ZView program that was made up of a resistor connected in parallel with a capacitor. From the fitting of the semi-circle to this model, we determine the conductivity of a sample. This "impedance spectroscopy" approach is critical when there is a mechanism of charge build-up. When electric charge is built-up somewhere in the sample (or at the electrode), electric response of a sample to applied voltage includes capacitance as well as resistance. In order to make correction for the capacitance effect, it is necessary to analyze the data from a broad frequency range. However, in some studies (e.g., Katsura et al., 1998; Yoshino et al., 2006, 2008a,b), they only adopt one frequency (0.01 Hz, in most case) to calculate the sample's electrical conductivity. Therefore in order to see the consequence of different methods of determining the conductivity, we have also calculated the conductivity from single frequency (0.01 Hz). Typical results of impedance spectroscopy are shown in Fig. 3.

In most of the runs, the conductivity was determined with decreasing temperature after the peak temperature was reached. However, in a few runs, the measurements of conductivity were made both with decreasing and increasing the temperature in order to test the hysteresis. Fig. 4 shows the results for a sample with high water content. We found no large hysteresis suggesting that the conductivity that we measure represents nearly equilibrium value for a given physical and chemical conditions at each measurement.

In order to assess the possible influence of leak current through an alumina piece surrounding a sample, we have made a measurement of "background resistivity". In this background test, a sample was replaced with an $Al_2O_3$ disc with the dimension of Ø 1.6 mm × 0.4 mm and the resistance of this material was measured at $P = 8.0$ GPa and $T = 873$–$1273$ K. We found that the resistance (calculated from the measured resistivity and the geometry of the sample) of an $Al_2O_3$ disc is ~$10^3$ times higher than anhydrous samples and more than ~$10^5$ times higher than for hydrous samples. We conclude that the influence of leak current is minimal under our experimental conditions.

All experimental conditions including before and after experimental water content, pressure and temperature are summarized in Table 2.

## 3. Results

The representative impedance spectroscopy results at conditions of 8.0 GPa, 873–1273 K and water content of 0.0046 wt% is shown in Fig. 3. Results obtained under other conditions are similar to those illustrated. We observed two circles at high temperatures, whereas only one circle was observed at low temperatures. The presence of two circles in the impedance spectroscopy implies two processes of charge transfer and blocking. The first circle originated at the origin ($Z' = Z'' = 0$) corresponds to a parallel combination of resistor and capacitor, and the second circle likely represents some processes including the interaction of charge species with elec-

**Table 2**
Summary of runs (>X).

| Run no. | $P$ (GPa) | $T$ (K) | Water content (H/$10^6$ Si) | |
|---|---|---|---|---|
| | | | Before experiment | After experiment |
| K707 | 4 | 873–1473 | >8 | >7 |
| K750 | 6 | 873–1473 | >9 | >7 |
| K753 | 8 | 873–1473 | >5 | >8 |
| K755 | 10 | 873–1473 | >7 | >4 |
| K758 | 14 | 873–1473 | >5 | >9 |
| K759 | 16 | 873–1473 | >10 | >9 |
| K767 | 8 | 873–1273 | 685 | 649 |
| K768 | 8 | 873–1273 | 2426 | 2385 |
| K782 | 8 | 873–1273 | 6898 | 6831 |
| K783 | 4 | 873–1273 | 685 | 657 |

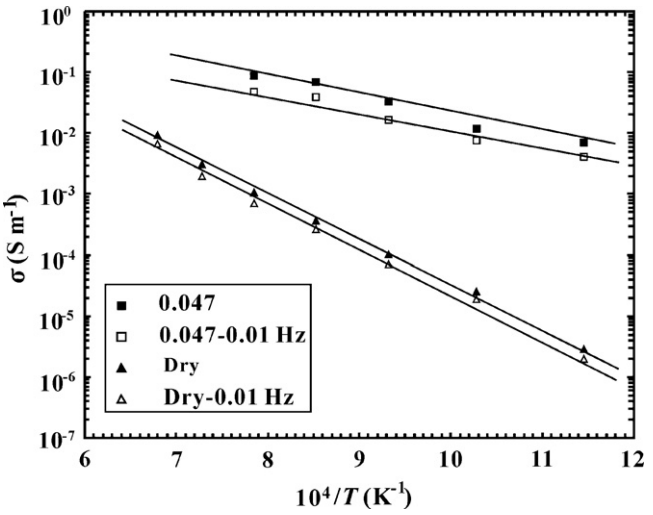


**Fig. 5.** Influence of method of calculation of electrical conductivity. The results from impedance analysis from the semi-circle fit are compared with the results based on single frequency (0.01 Hz) fit. Results from dry and from hydrous pyrope (0.047% water) are shown (at 8 GPa, 873–1273 K).

trodes (Huebner and Dillenburg, 1995; Barsoukov and Macdonald, 2005). The presence of a capacitor in the impedance response implies that there is a mechanism to accumulate electric charge in the sample. Since our samples are single crystals, the most likely mechanism for charge accumulation is the time-dependent reaction at the electrode (Tyburczy and Roberts, 1990). When charge is transferred from a sample to an electrode, an electron must be transferred to a wire in order to maintain the electric current. If this transfer takes a finite time comparable to or larger than the inverse frequency of the voltage, then charge will be accumulated at the electrode that will give rises to a capacitor.

If this interpretation is correct, then the "resistance" that one determines at low frequencies (away from the first circle) will not provide us with the correct electrical conductivity (resistivity). In order to show this point, we plot the calculated conductivity by two different methods: one from the fitting of the impedance spectroscopy results and another from the frequency = 0.01 Hz point (Fig. 5). Although differences are not large for these samples, systematic differences are observed and we used the results from the impedance fitting.

The electrical conductivity of the samples were calculated using the following equation:

$$\sigma = \frac{L/S}{R} = \frac{L}{SR} \tag{2}$$

where $L$ is the sample thickness and $S$ is the cross-section area of the electrode.

Electrical conductivity of a mineral containing both the ferric iron and hydrogen can be expressed as:

$$\sigma = \sigma_{Fe} + \sigma_H \tag{3}$$

where $\sigma_{Fe}$ is the electrical conductivity due to ferric iron, $\sigma_H$ is the electrical conductivity due to hydrogen. $\sigma_{Fe}$ and $\sigma_H$ may be expressed as, respectively:

$$\sigma_{Fe} = A_{Fe} \exp\left(-\frac{H^*_{Fe}}{RT}\right) \tag{4}$$

$$\sigma_H = A_H C_w^r \exp\left(-\frac{H^*_H}{RT}\right). \tag{5}$$

$\sigma_{Fe}$ and $\sigma_H$ are electrical conductivity due to ferric iron and proton, the $A_{Fe}$, $A_H$ and $r$ are constants, the $H^*_{Fe}$ and $H^*_H$ are the activation enthalpies corresponding to these two mechanisms, $R$ is the gas constant and $T$ is temperature with

$$H^* = E^* + P \cdot V^* \tag{6}$$

where $P$ is pressure.

**Table 3**
Parameter values for the electrical conductivity of pyrope-rich garnet (units: $A$: S/m, $E^*$: kJ/mol, $V^*$: cm$^3$/mol, $P$: GPa). The relation $\sigma = A \cdot C_w^r \exp(-(E^* + PV^*)/RT)$ and $\sigma = A \cdot \exp(-(E^* + PV^*)/RT)$ are used for wet conditions and dry conditions respectively. Under dry conditions, the experimental data show strong dependence of $A$ on pressure. Therefore we used a relation $A = A_o\ (1 - B{\cdot}P)$ or $A = \exp\ [C_o(1 - D{\cdot}P)]$ (B and D in 1/GPa). Under wet conditions, the pressure dependence of $A$ is not well-constrained, and we assumed a pressure-independent $A$. Errors are one standardized deviation, and include the contribution of errors in individual measurements (errors in water content, temperature and electrical conductivity).

| | $A$ | $r$ | $E^*$ | $V^*$ |
|---|---|---|---|---|
| Wet | 1950 (+870, −600) | 0.63 ± 0.19 | 70 ± 5 | −0.57 ± 0.05 |
| Dry | $A_o$ = 1036(±236)<br>$B$ = 0.044(±0.007)<br>$C_o$ = 7.16(±0.37)<br>$D$ = 0.012(±0.009) | – | 128 ± 6 | 2.50 ± 0.48 |

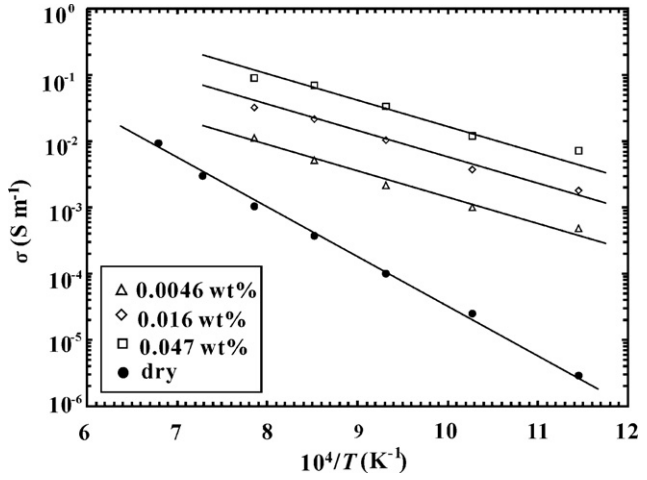


**Fig. 6.** Electrical conductivity for garnet versus inverse temperature relationship at $P$ = 8 GPa and $T$ = 873–1473 K for different water contents.

Fig. 6 shows

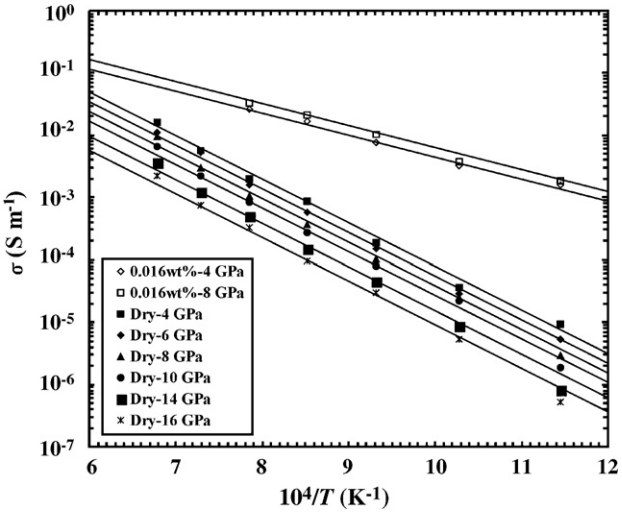


**Fig. 7.** Influence of pressure on the electrical conductivity of garnet at the temperature of 873–1473 K.

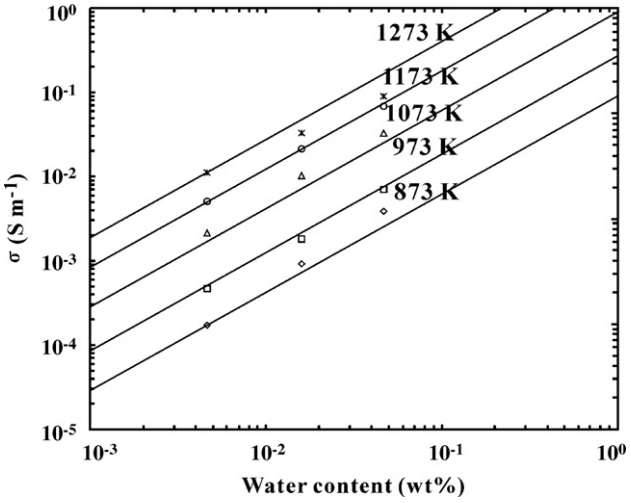


**Fig. 8.** Electrical conductivity versus water content relationship for hydrous garnet under conditions of 8 GPa and 873–1273 K.

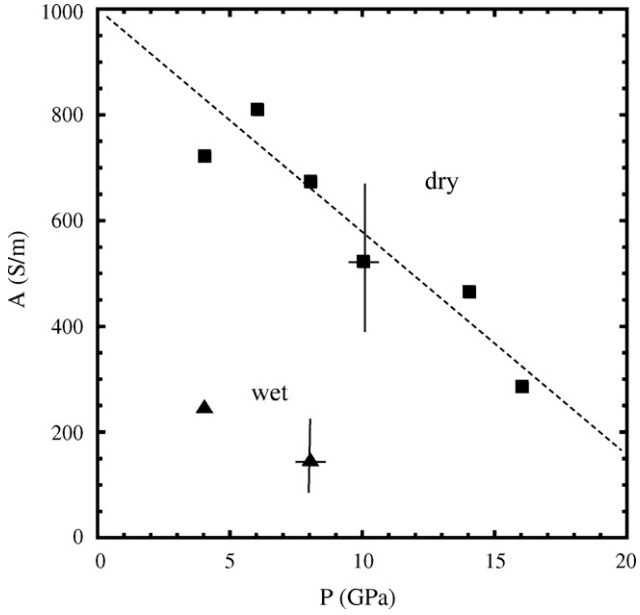


**Fig. 9.** The pressure dependence of pre-exponential factor, $A$. The pre-exponential factor under dry conditions shows strong pressure dependence, whereas the pressure dependence under wet conditions is not well resolved. The pressure dependence under dry conditions was analyzed using either $A = A_o(1 - B{\cdot}P)$ or $A = \exp[C_o(1 - D{\cdot}P)]$ where $A_o$, $B$ and $C_o$ and $D$ are constants.

the influence of temperature and water content at $P = 8$ GPa. Fig. 7 shows the influence of pressure. The results from impedance analysis from the semi-circle fit are compared with the results based on single frequency (0.01 Hz) fit for a dry and for a hydrous pyrope-rich granet (0.016 wt% water). Fig. 8 shows the relation between electrical conductivity and water content under the conditions of 8 GPa and 873–1273 K.

## 4. Summary and discussions

We have obtained an extensive data set on the electrical conductivity of single crystal pyrope-rich garnet under the controlled oxygen fugacity and water (hydrogen) content for a broad range of pressure and temperature. We determined the electrical conductivity through the impedance spectroscopy by fitting an equivalent circuit model for the first $Z'$–$Z''$ semi-circle. We also estimated an effective conductivity using only one frequency (0.01 Hz) to examine the influence of different methods. We found that there are systematic differences in estimated electrical conductivity by these two different methods: results from one low frequency (0.01 Hz) show systematically lower conductivity that results from the impedance spectroscopy fit, and the difference becomes large as water content increases. These differences are the artefact caused by some processes that block electric current (e.g., electrode reaction) and consequently both the magnitude and the activation enthalpy determined from single frequency do not correspond to true material properties.

We have identified two distinct mechanisms of electrical conductivity. Under anhydrous condition, electrical conductivity is less than that under hydrous conditions, and the activation enthalpy is higher under anhydrous conditions than that under hydrous conditions (there is no detectable dependence of activation enthalpy on water content under hydrous conditions). Under anhydrous conditions, electrical conduction occurs by a mechanism with relatively high activation enthalpy and decreases slightly with pressure. We also found that the pre-exponential term decreases significantly with pressure under dry (anhydrous) conditions (Fig. 9) (such a trend is unclear for wet conditions, and the pressure dependence of pre-exponential term was never been determined for minerals such as olivine (e.g., Xu et al. (2000) analyzed the data on olivine assuming that the pre-exponential term is independent of pressure). Such a strong pressure dependence of pre-exponential factor is not expected for ionic conduction (e.g., Mott and Gurney, 1948). Consequently, we consider that the strong pressure dependence is due to the pressure dependence of some electronic properties of this material including the pressure dependence of energy band structure and/or an impurity state (ferric iron state) in the band gap (e.g., Bosman and van Daal, 1970).

In summary, we suggest that electrical conduction under anhydrous conditions is likely due to electronic defects including a "small polaron" as shown in olivine (Schock et al., 1989). Electrical conductivity under hydrous conditions depends on hydrogen content and has a smaller activation enthalpy. The dependence of conductivity on hydrogen content and the activation enthalpy for pyrope-rich garnet are similar to those found in olivine and wadsleyite (Wang et al., 2006; Huang et al., 2005). Therefore we interpret that the electrical conductivity in pyrope-rich garnet under hydrous conditions likely occur through the charge transfer by some hydrogen-related defects such as "free" proton or proton trapped at vacant lattice site.

Our results can be compared with those by Romano et al. (2006) where electrical conductivity of synthetic pyrope-almandine was measured to 19 GPa. The results by Romano et al. (2006) for $Py_{85}$-$Alm_{15}$ at 10 GPa agree well with ours, but the results by Romano et al. (2006) for $Py_{85}$-$Alm_{15}$ at 19 GPa are considerably different from ours. In general, Romano et al. (2006) reported that the electrical conductivity of pyrope-almandine increases with pressure, whereas our results show that the electrical conductivity of pyrope-rich garnet decreases with pressure under anhydrous conditions, whereas the addition of water (hydrogen) enhances conductivity and the activation enthalpy under hydrous conditions is smaller than that under anhydrous conditions. The results of Romano et al. (in particular for $Py_{85}$-$Alm_{15}$) show that electrical conductivity of their sample is higher at higher pressures and the activation enthalpy is smaller at higher pressures. These results are different from ours, and a possible reason for this discrepancy is the possible difference in water content (an alternative explanation is that the ferric iron content may increase with pressure, but electrical conduction by ferric iron (i.e., "small polaron") generally has a higher activation energy than reported by Romano et al. (2006)). However, because water content was not measured in Romano et al. (2006)'s

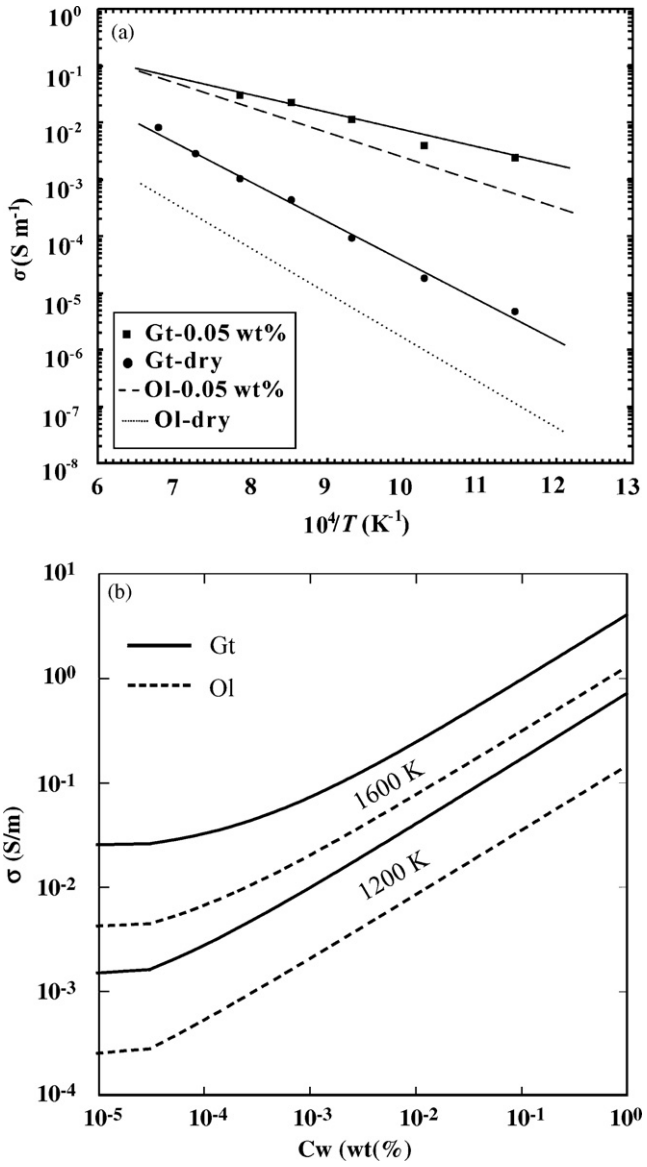


**Fig. 10.** A comparison of electrical conductivity of (pyrope-rich) garnet with that of olivine. Comparison is made at $P = 4$ GPa and for the same Fe# (Fe/(Fe + Mg + Ca)). The olivine data are from Xu et al. (2000) and Wang et al. (2006).

study, it is difficult to draw any definitive conclusions as to the cause of this difference.

We compare the electrical conductivity of pyrope with that of olivine. The comparison is made at the same Fe# = Fe/(Mg + Fe + Ca) ratio (Fig. 10a). The results show that under water-free (dry) conditions, pyrope garnet has about 10 times higher conductivity than olivine at the same Fe#, whereas pyrope has only slightly higher conductivity at water-rich (wet) conditions. In order to compare the electrical conductivity between olivine and pyrope in the deep upper mantle conditions, we have made corrections for Fe and H partitioning using the experimental data by Irifune and Isshiki (1998) and Mookherjee and Karato (in press). The experimental data by Romano et al. (2006) are used to make corrections for the effect of Fe# for pyrope and the present results were used to make the corrections for hydrogen content. Fig. 10b compares the electrical conductivity of co-exiting pyrope-rich garnet and olivine at $P = 4$ GPa, $T = 1200$ and 1600 K as a function of water content. We find that pyrope-rich garnet has ~10 times higher electrical conductivity than co-existing olivine under these conditions. The actual contribution from garnet depends not only its volume fraction but also its geometry. When garnet is connected (above the percolation threshold), then its contribution to electrical conductivity is large. The percolation threshold is ~0.2–0.3 (e.g., Stauffer and Aharony, 1992) and therefore for a range of volume fraction of garnet, its contribution is marginally important in a typical upper mantle (volume fraction is 0.1–0.2), but its contribution is very important in a garnet-rich region such as subducted oceanic crust in the deep mantle (volume fraction is ~0.9: Irifune and Ringwood, 1987) or piclogite rich regions (~0.5–0.8: Bass and Anderson, 1984).

## Acknowledgements

We thank Mainak Mookherjee, Zhicheng Jing and Zhenting Jiang for the technical assistance. Justin Hustoft made several corrections of English. This research is financially supported by the NSF of China and the NSF of the United States.

## References

Barsoukov, E., Macdonald, J.R., 2005. Impedance Spectroscopy Theory, Experiment, and Applications (Second Edition). John Wiley & Sons, Inc, pp. 17–129.
Bass, J.D., Anderson, D.L., 1984. Composition of the upper mantle: geophysical test of two petrological models. Geophys. Res. Lett. 11, 237–240.
Bosman, A.J., van Daal, H.J., 1970. Small-polaron versus band conduction in some transition-metal oxides. Adv. Phys. 19, 1–117.
Huang, X.G., Xu, Y.S., Karato, S., 2005. Water content in the transition zone from electrical conductivity of wadsleyite and ringwoodite. Nature 434, 746–749.
Huebner, J.S., Dillenburg, R.G., 1995. Impedance spectra of dry silicate minerals and rock: qualitative interpretation of spectra. Am. Miner. 80, 46–64.
Irifune, T., Ringwood, A.E., 1987. Phase transformations in primitive MORB and pyrolyte composition to 25 GPa and some geophysical implications. In: Manghnani, M.H., Syono, Y. (Eds.), High-Pressure Research in Mineral Physics. American Geophysical Union, Washington, DC, pp. 231–242.
Irifune, T., Isshiki, M., 1998. Iron partitioning in a pyrolite mantle and the nature of the 410-km seismic discontinuity. Nature 392, 702–705.
Karato, S., 1990. The role of hydrogen in the electrical conductivity of the upper mantle. Nature 347, 272–273.
Karato, S., Dai, L. Comments on "Electrical conductivity of wadsleyite as a function of temperature and water content" by Manthilake et al. Phys. Earth Planet. Inter., in press, doi:10.1016/j.pepi.2009.01.011.
Katsura, T., Sato, K., Ito, E., 1998. Electrical conductivity of silicate perovskite at lower-mantle conditions. Nature 395, 493–495.
Mookherjee, M., Karato, S. The solubility of water in pyrope garnet. Chem. Geol., submitted for publication.
Morishima, H., Kato, T., Suto, M., Ohtani, E., Urakawa, S., Utsumi, W., Shimomura, O., Kikegawa, T., 1994. The phase boundary between α- and β-$Mg_2SiO_4$ determined by in situ X-ray observation. Science 265, 1202–1203.
Mott, N.F., Gurney, R.W., 1948. Electronic Processes in Ionic Crystals (Second Edition). University Press, Oxford, pp. 274.
Paterson, M.S., 1982. The determination of hydroxyl by infrared absorption in quartz, silicate glasses and similar materials. Bull. Miner. 105, 20–29.
Ringwood, A., 1975. Composition and Petrology of the Earth's Mantle. McGraw-Hill, New York, 618 pp.
Romano, C., Poe, B.T., Kreidie, N., McCammon, A., 2006. Electrical conductivities of pyrope-almandine garnets up to 19 GPa and 1700 °C. Am. Miner. 91, 1371–1377.
Schock, R.N., Duba, A.G., Shankland, T.J., 1989. Electrical conduction in olivine. J. Geophys. Res. 94, 5829–5839.
Stauffer, D., Aharony, A., 1992. Introduction to Percolation Theory. Taylor and Francis, pp. 181.
Tyburczy, J.A., Roberts, J.J., 1990. Low frequency electrical response of polycrystalline olivine compacts: grain boundary transport. Geophys. Res. Lett. 17, 1985–1988.
Wang, D.J., Mookherjee, M., Xu, Y.S., Karato, S., 2006. The effect of water on the electrical conductivity of olivine. Nature 443, 977–980.
Xu, Y., Shankland, T.J., Duba, A., 2000. Pressure effect on electrical conductivity of mantle olivine. Phys. Earth Planet. Inter. 118, 149–161.
Yoshino, T., Matsuzaki, T., Yamashita, S., Katsura, T., 2006. Hydrous olivine unable to account for conductivity anomaly at the top of the asthenosphere. Nature 443, 973–976.
Yoshino, T., Manthilake, G., Matsuzaki, T., Katsura, T., 2008a. Dry mantle transition zone inferred from the conductivity of wadsleyite and ringwoodite. Nature 451, 326–329.
Yoshino, T., Nishi, M., Matsuzaki, T., Yamazaki, D., Katsura, T., 2008b. Electrical conductivity of majorite garnet and its implications for electrical structure in the mantle transition zone. Phys. Earth Planet. Inter. 170, 193–200.
Zhang, J., Li, B., Utsumi, W., Liebermann, R.C., 1996. In situ X-ray observations of the coesite-stishovite transition: reversed phase boundary and kinetics. Phys. Chem. Miner. 23, 1–10.